Journal of Achievements in Materials and Manufacturing Engineering
VOLUME 36
ISSUE 1
September
2009

Influence of LCVD technological parameters on properties of polyazomethine thin films

B. Hajduk [a,b,*], J. Weszka [a,b], J. Jurusik [b]

[a] Division of Materials Processing Technology, Management and Computer Techniques in Materials Science, Institute of Engineering Materials and Biomaterials, Silesian University of Technology, ul. Konarskiego 18a, 44-100 Gliwice, Poland

[b] Department of Physics, Center of Polymer and Carbon Materials, Polish Academy of Sciencies, ul. M. Curie-Sklodowskiej 34, 41-819 Zabrze, Poland

* Corresponding author: E-mail address: b.hajduk@cmpw-pan.edu.pl

Received 21.02.2009; published in revised form 01.09.2009

Properties

ABSTRACT

Purpose: The aim of this paper is to show influence of technological parameters (temperature and gas stream intensity) of low-temperature chemical vapour deposition (LCVD) on optical properties and morphology of polyazomethine thin films.

Design/methodology/approach: Thin layers of poly (1,4-phenylene-methylenenitrilo-1,4-phenylenenitrilo-methylene) (PPI) were prepared by low temperature LCVD method with use of argon as a transport agent. The UV-Vis spectroscopy and AFM microscopy measurements on PPI thin films were performed.

Findings: The LCVD parameters, like temperature and argon stream intensity, influence growth rate, morphology and optical properties of polyazomethine thin films. Optimalization of technical parameters allows for thin films with desired properties to be prepared.

Research limitations/implications: Optimalization of technical LCVD parameters leads to preparing PPI thin films having desired morphology and optical properties suitable for optoelectronic applications.

Practical implications: PPI polyazomethine is good material for potential applications as the active layer in optoelectronic or photonic structure (diods or photovoltaic cells).

Originality/value: LCVD with use of argon is relatively new method for preparing of thin polymer films. Recognizing of optimal technical parameters will make possible getting of thin films with required properties.

Keywords: UV-Vis spectroscopy; AFM microscopy; LCVD; Conjugated polymer

Reference to this paper should be given in the following way:

B. Hajduk, J. Weszka, J. Jurusik, Influence of LCVD technological parameters on properties of polyazomethine thin films, Journal of Achievements in Materials and Manufacturing Engineering 36/1 (2009) 41-48.

1. Introduction

Low-temperature chemical vapor deposition (LCVD) [1-5] is one of CVD methods [6-8] and has appeared to be a very useful method for preparing thin films poly (1,4-phenylenemethylenenitrilo-1,4pheny-lenenitrilomethylene) (PPI) [9-12]. PPI thin films grown under various technological conditions of LCVD process are of very high technical purity and free from unintentional impurities. It has been found that surface morphology and optical properties of PPI thin films are very sensitive on such technological conditions of LCVD process as: the intensity of Ar stream flow, p-phenylenediamine (PPDA) and terepthal aldehyde (TPA) temperatures, T_{PPDA} and T_{TPA}, respectively, as well as their difference $\Delta T = T_{PPDA} - T_{TPA}$. To verify how these parameters can be used to control LCVD process of preparing PPI thin films with desired properties four series of experiments were carried out. In all these experiments the time of the film deposition and set-up geometry and T_{PPDA} and the substrate room temperature were fixed and constant.

The series were diversified by ratio of the source temperatures or more precisely by their difference ΔT, which were changed with 10^0C increment within the range 0 – 30 °C. Then, PPI thin films were deposited under different argon stream flow intensity in each series. The aim of this paper is to show how technical parameters influence optical properties and morphology of PPI thin films and how to determine optimal parameters to get thin films with desired properties [14], without disadvantages in absorption spectrum and AFM topographic images. Our interest in polyazomethine PPI thin films results from its being isoelectronic counterpart of polyparaphenylene-vinylene (PPV) [13].

2. Materials and technology

Polyazomethine thin films were prepared by LCVD method based on polycondensation of p-phenylene diamine (PPDA) and terphtal aldehyde (TPA) with argon used as a transport agent. The stream of argon was forked into three equal streams (Fig.1), which flow around crucibles containing two monomers. Then, two streams merged into one stream of mixed monomers and argon molecules in the stream collimator, so that there was one stream transporting all mixed molecules towards the glass substrate. While preparing pristine PPI thin films two sources were used only, the third crucibles was empty. Five microscope glass substrates were placed onto rotary plate (Fig. 1).

PPDA and TPA molecules impinging onto the substrate kept at room temperature can be adsorbed or come back to vapor phase. Within the adsorption layer molecules jump, stick each other starting the polycondensation reaction, as shown in Fig. 2, resulting in HC=N bonds formation and polyazomethine chain elongation, which is associated with releasing one water molecule at each step. Four series of LCVD deposition processes of PPI thin films were carried out under low vacuum of about 10^{-1}Tr. Technical parameters of all series of the deposition processes are given in Table 1. Each series has consisted of five processes during which thin films were deposited under five various argon stream flow intensities and deposited thin films are designated a, b, c, d and e, respectively. In each series subsequent films were deposited onto room temperature glass substrate with higher and higher intensity of argon stream during 2 min long deposition process.

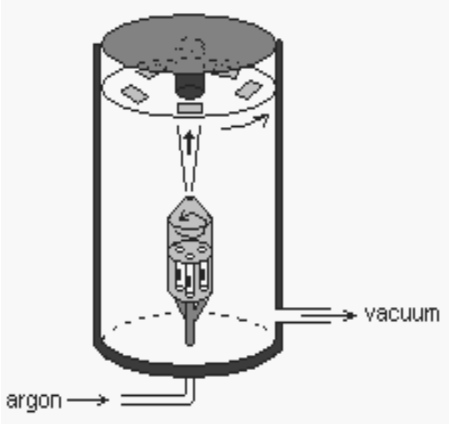

Fig. 1. LCVD setup

Table 1.
Technical parameters of individual experiments

No	T_{TPA}/T_{PPDA} [°C]	I [Tr*l/s]	t [min]
1(a,b,c,d,e)	50/50	0.05(a) / 0.15(b) / 0.4(c) / 1(d) / 3(e)	2
2(a,b,c,d,e)	50/60		2
3(a,b,c,d,e)	50/70		2
4(a,b,c,d,e)	50/80		2

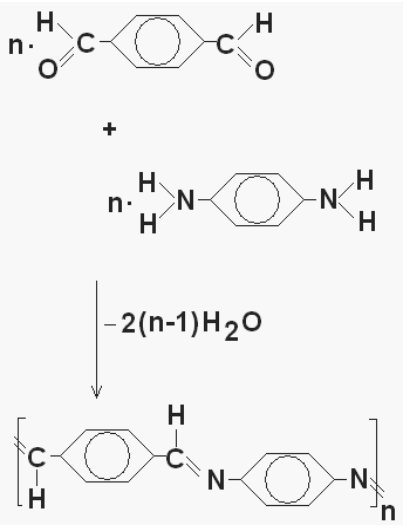

Fig. 2. Polycondensation of pol(1.4-phenylenemethylenenitrilo-1.4phenylenenitrilomethylene)

The thickness of the as-prepared thin films was in 20 - 2000 nm interval, depending on the intensity of the stream of gas and monomers molecules. Measurements of thickness were taken by Tolanski method with the interference microscope using yellow light. The thickness of every thin film was calculated by equation:

$$d = \frac{\lambda}{2} \cdot \frac{\Delta L}{L} \text{ [Å]} \quad (1)$$

where:
d- thickness of layer [nm]
λ – wavelength [nm]
L – interval between stripes
ΔL – relocalization of stripe

Optical UV-VIS absorption spectra were recorded with Ocean optics HR4000 spectrophotometer within 200 – 1000 nm wavelength interval. The topographic images of surface morphology of the as-prepared PPI thin films were taken with Atomic Forces Microscope (AFM). All measurements were performed at room temperature.

3. Results

3.1. UV-VIS measurements

UV-VIS optical absorption spectra versus photon energy recorded for all the PPI thin films series are shown in Figs. 3-6. In each figure, there are shown spectra of five PPI thin films belonging to one series, which were prepared with various flow rates. The series illustrated in consecutive figures were performed for larger differences between PPDA and TPA monomers temperature ΔT increased with an increment of 10°C.

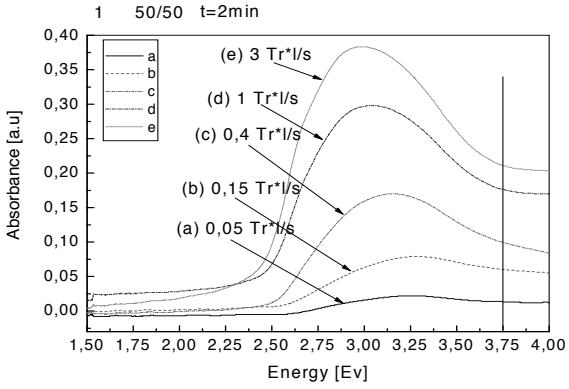

Fig. 3. UV-Vis spectra of PPI layers prepared with equal temperature of monomers, ΔT= 0°C

As it is seen in Table 1, the first series was prepared with the same temperatures of monomers (ΔT=0) (Fig. 7). The films whose spectra are shown in Figs 4-6 were prepared under ΔT equal to 10, 20 and 30^0C, respectively. The values of gas stream intensity while preparing successive thin films are shown in every figure.

Technological parameters applied during deposition of each series of PPI thin films, such as T_{PPDA} and T_{TPA} temperatures (e.g. temperature of TPA/ temperature of PPDA = 50/50) and time elapsed during the deposition process of each thin film are visible above every graph. It can be seen in the first three figures (Figs. 8-10) that the increase in the absorption intensity is not associated with any change in the shape of spectrum. However, one can see in Fig. 6 that not only the absorption intensity increases but also the shape of spectrum changes when the stream intensity is increasing. One can see in all the spectra that the absorption intensity is the higher the higher intensity of the stream is. The perpendicular line in each of Figs. 3-6 and Figs. 9-12 drawn at 3.75 eV photon energy is used because in this area the shape of the spectra is the same and absorption level is influenced by film thickness only.

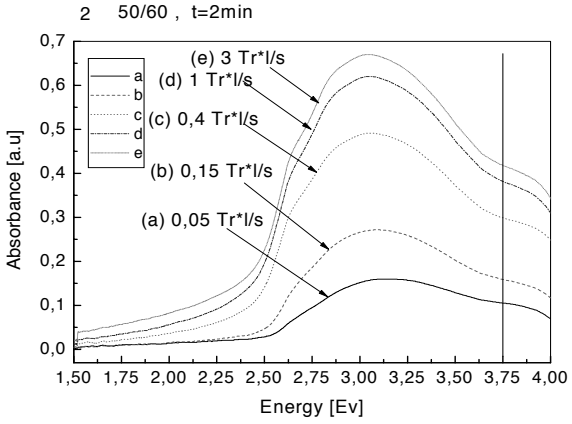

Fig. 5. UV-Vis spectra of PPI prepared with 10°C difference between monomer's temperature

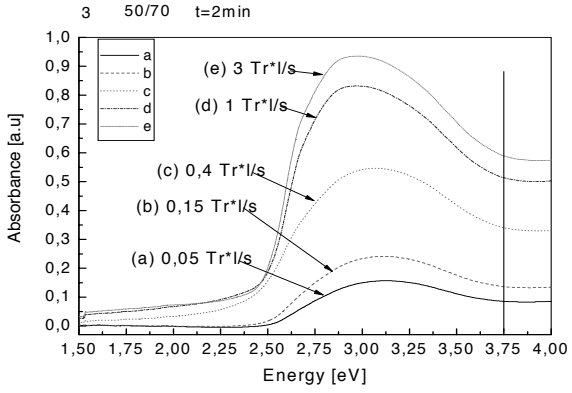

Fig. 4. UV-Vis spectra of layers prepared with 20 °C difference between monomer's temperature

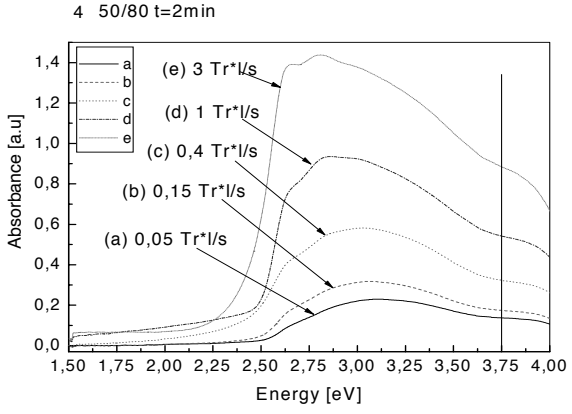

Fig. 6. UV-Vis spectra of PPI layers prepared with 30 °C difference between monomer's temperature

3.2. AFM measurements

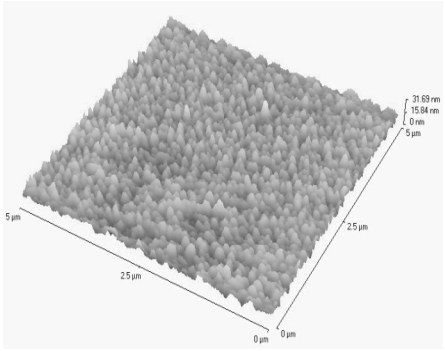

ΔT = 0 deg, I= 0.05 Tr*l/s (a)

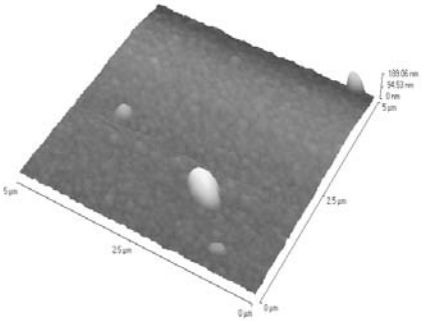

ΔT = 0 deg , I= 0.15 Tr*l/s (b)

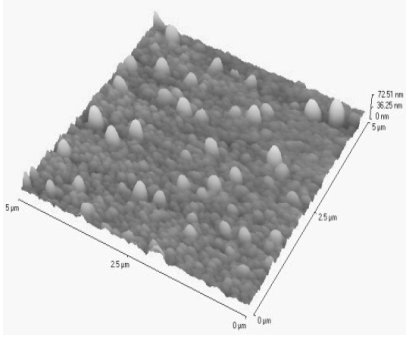

ΔT = 0 deg , I = 0.4 Tr*l/s (c)

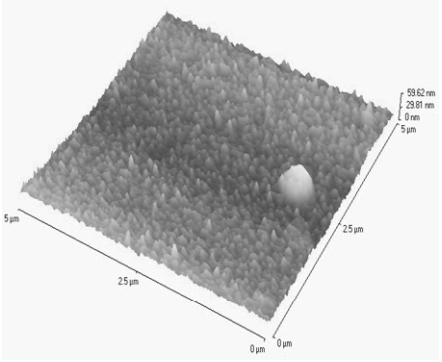

ΔT = 0 deg, I = 1 Tr*l/s (d)

Fig. 7. Topographic images of series 1, prepared with ΔT =0 °C and with increasing Ar stream intensity

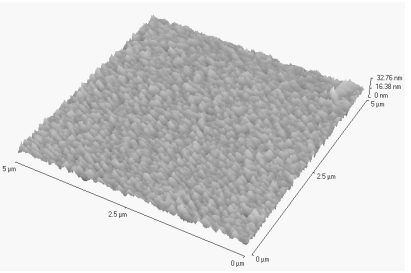

ΔT = 10 deg, I= 0.05 Tr*l/s (a)

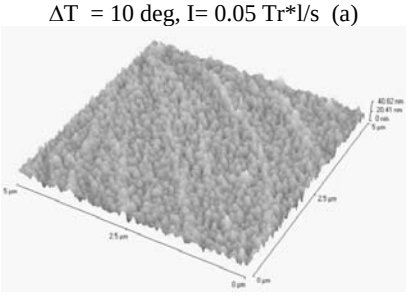

ΔT = 10 deg , I= 0.15 Tr*l/s (b)

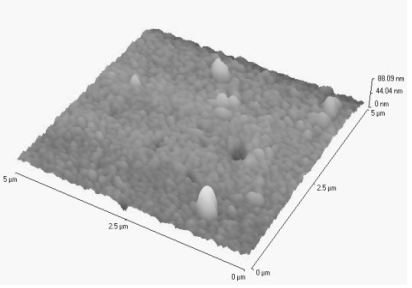

ΔT = 10 deg , I = 0.4 Tr*l/s (c)

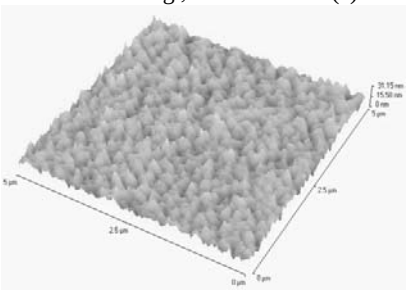

ΔT = 10 deg, I = 1 Tr*l/s (d)

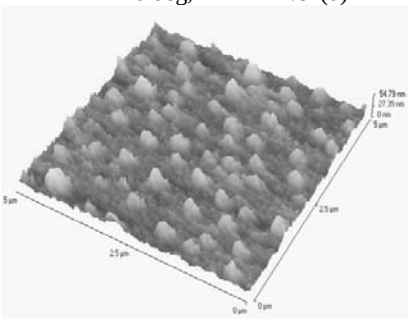

ΔT = 10 deg, I = 3 Tr*l/s (e)

Fig. 8. Topographic images of series 2, prepared with ΔT =10 °C and with increasing Ar stream intensity

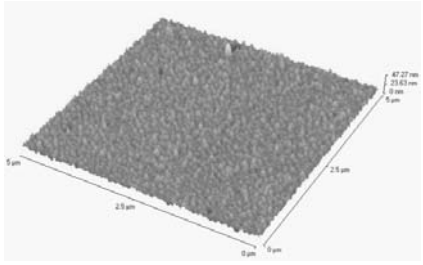

ΔT =20 deg, I= 0.05 Tr*l/s (a)

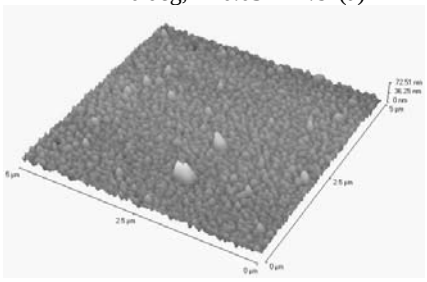

ΔT =2 0 deg , I= 0.15 Tr*l/s (b)

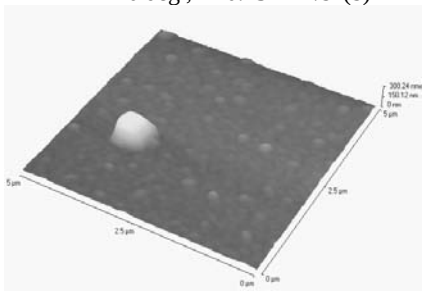

ΔT = 20 deg , I = 0.4 Tr*l/s (c)

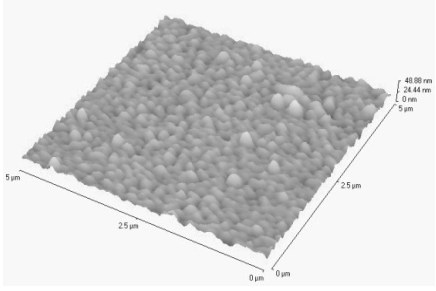

ΔT = 20 deg, I = 1 Tr*l/s (d)

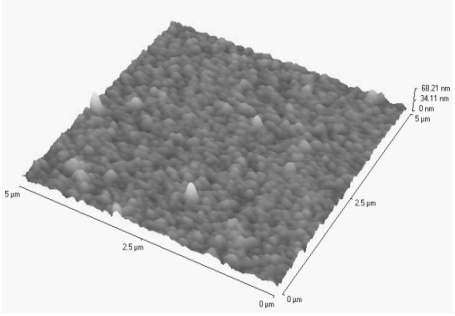

ΔT = 10 deg, I = 3 Tr*l/s (e)

Fig. 9. Topographic images of series 3, prepared with ΔT =20°C and with increasing Ar stream intensity

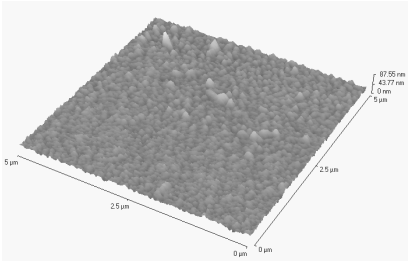

ΔT =30 deg, I= 0.05 Tr*l/s (a)

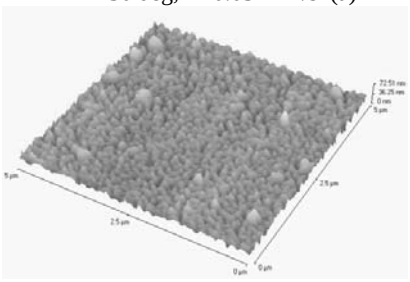

ΔT =30 deg , I= 0.15 Tr*l/s (b)

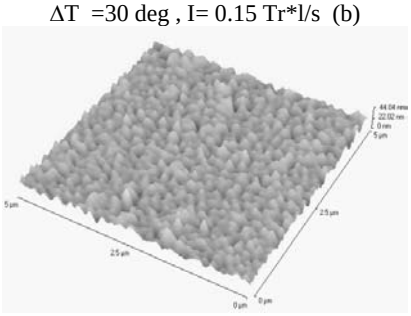

ΔT = 30 deg , I = 0.4 Tr*l/s (c)

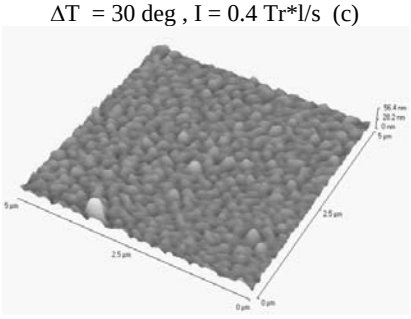

ΔT = 30 deg, I = 1 Tr*l/s (d)

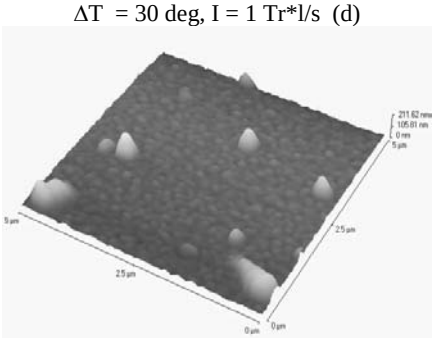

ΔT = 30 deg, I = 3 Tr*l/s (e)

Fig. 10. Topographic images of series 4, prepared with ΔT =30°C and with increasing Ar stream intensity

The topographic images of 5x5 μm were performed in contact mode with Atomic Forces Microscope at room temperature. Thopographic images for subsequent series are arranged with increasing Ar intensity (0.05Tr*l/s (a), 0.15 Tr*l/s (b), 0.4 Tr*l/s (c), 1Tr*l/s (d) and 3 Tr*l/s (e)) and are shown in. Figs. 7-10. Single big grains and holes are seen in some topographic images. An egzample average diameter of big grains in Fig. 8c) is 0.62 μm and depth of surface hole is 0.60 μm.

4. Discussion

Topographic images of thin PPI films were treated in terms of applied technological parameters: "I" – gas stream intensity, "ΔT"- difference of monomers temperature and "V" growth rate of thin films, which depends itself on I and ΔT. Thickness of all films are known and are shown in Table 3. One can see, in Table 3, that growth rate V was increasing with I gas stream intensity and ΔT, the latter effect has appeared to be more pronounced. Thickness of subsequent films, prepared with equal deposition time t = 2 min was increasing with an increase of growth rate V. To characterise roughness of polymer surface morphology the RMS coefficients were used, where RMS coefficient (Root Mean Square roughness) [15] is defined as:

$$RMS = \sqrt{\frac{1}{n} \cdot \sum_{i=1}^{n} (Z_i - \overline{Z})^2} \quad [\text{nm}] \qquad (2)$$

were n is the number of sampled points, Z_i is the height of each point and $\overline{Z}$ is the mean height value. RMS coefficients of most films are in range 2.3 – 6.5 nm, but those from several films revealing surface with scattered big grains have appeared to be higher than 7 nm. It is noticeable that the size of individual grains was growing up for subsequent films. The films belonging to Series No.2 are make an example of such change:

Table 2.
Values of intensity I and grain size S

No.	2 a)	2 b)	2 c)	2 d)	2 e)
I (Tr*l/s)	0.05	0.15	0.40	1.00	3.00
S (μm)	0.14	0.15	0.16	0.19	0.22

One can see, that grain size S is increasing with growing argon stream intensity. In fact, the rise of argon stream intensity influences morphology of polymer surface. The surface of polymer thin film prepared with low intensity, I = 0.05 Tr*l/s, is regularly granular with grain boundaries being clearly visible. The increase of gas stream intensity to I = 0.15 Tr*l/s caused no significant changes in film surface morphology, though one can see boundaries between grains more widened and the nearest neighbour grains are seen to coalesce into one grain, the grain size becoming larger. Further rise of gas stream intensity caused appearing of big grains scattered on thin film surface with simultaneous surface flattening between them. Big grains are attributed to more ordered areas in PPI thin film structure due to aggregation of polymer chains.

The influence of technological conditions on films properties observed in UV-Vis spectra is seen to correspond rather well with variations of their morphology recorded with AFM. Absorption measurements were performed at room temperature. The absorption spectra of PPI thin films series prepared under ΔT= 0 deg and ΔT = 30 deg, normalised at energy 3.75 eV, are shown in Fig. 12 and Fig. 13 respectively. Variations of the film growth rate versus the argon stream intensity I for various ΔT are shown in Fig. 11.

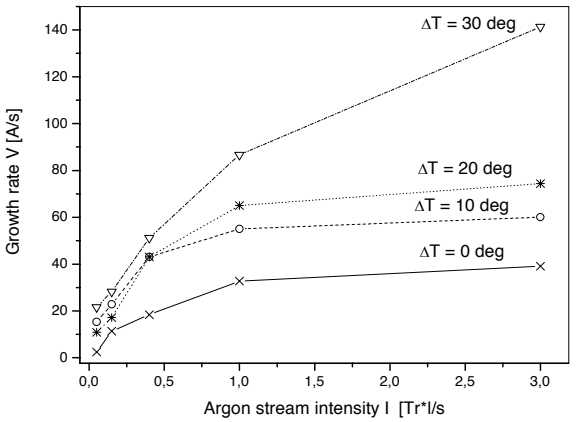

Fig. 11. Growth rate V dependence on technological conditions ΔT and I

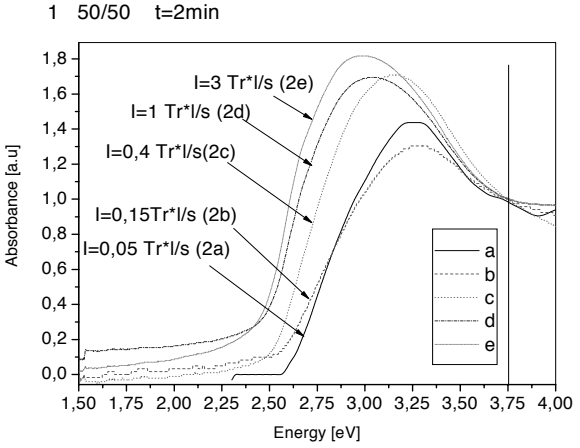

Fig. 12. Normalised spectra of PPI thin films prepared with equal monomer's temperature

One can see, that the growth rate V of PPI thin films depends on the argon stream I in a similar way, though it is more steeper for ΔT =30 deg. What is common for all serries, for the smallest streams the slop is the largest and decreases slightly with V increase up to 1 Tr*l/s. But the growth rate level is seen to be proportional to ΔT at each stage. However, one can see that for strems larger that 1 Tr*l/s the growth rate becomes neraly constant for ΔT equal to 0, 10 and 20 deg. In contrast, the growth rate V increases distinctly under ΔT =30 deg, being much larger for I = 3 Tr*l/s than for I = 1 Tr*l/s. The spectra given in Figs. 12 – 13 reveal some shift of their maxima towards lower energy with increasing argon stream intensity.

Additionally, the band shape variation with the stream flow rate is seen to be most visible when ΔT =30 deg. One can also see that the band maximum shifts from 3.27 eV for ΔT =0 deg

towards 3.1 eV for films prepared for ΔT =30 deg. Two films prepared under ΔT =0 with the lowest flow rates are seen to have their maxima at photon energy of about 3.25eV, while other spectra have their maxima at about 3.00 eV. It is expected that these shifts of maxima reflect variation of potential energy minima between the electron ground and excited states. Then, one can expect that the potential energy minimum of the excited state is less displaced from the ground state minimum (Fig. 14) for thin films prepared under ΔT =30deg. The observed displacement of the band towards lower energy with increased flow rate is thought to indicate an increase in conjugation length of PPI chains.

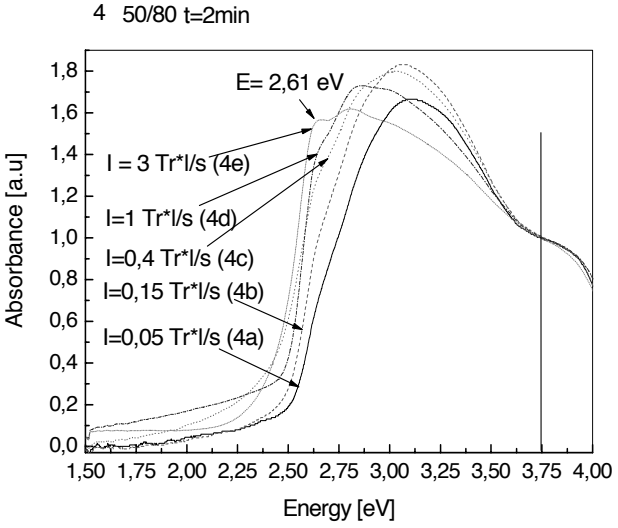

Fig. 13. Normalised spectra of PPI layers prepared under ΔT=20°C

This correspond rather well with the film growth rates V given in Table 2 and deduced dividing the film thickness (l) by the time of a film deposition (t). One can see, that shape of absorption band is changed in Fig. 13. Vibronic proggressions are seen in 4d) spectrum and additional peak is seen 2.61 eV, which is attributed to fomation of Wannier – Mott exciton states in PPI film. Wannier – Mott exciton is electrostatic connection of delocalised electron and delocalised hole. One can expect, that Wannier –Mott excitons are formed within a volume of the film where PPI chains aggregate.

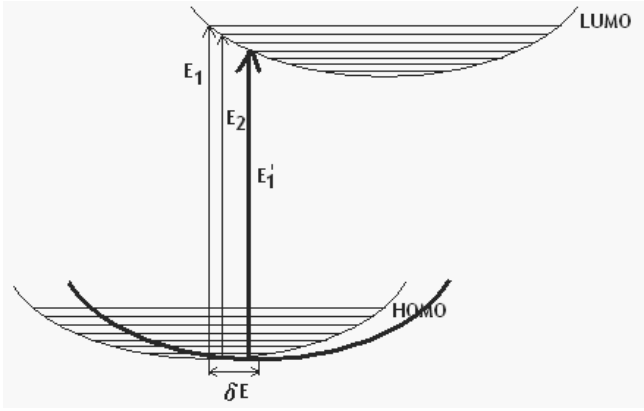

Fig. 14. Sample shift of LUMO state in PPI prepared with lower and higher growth rate V

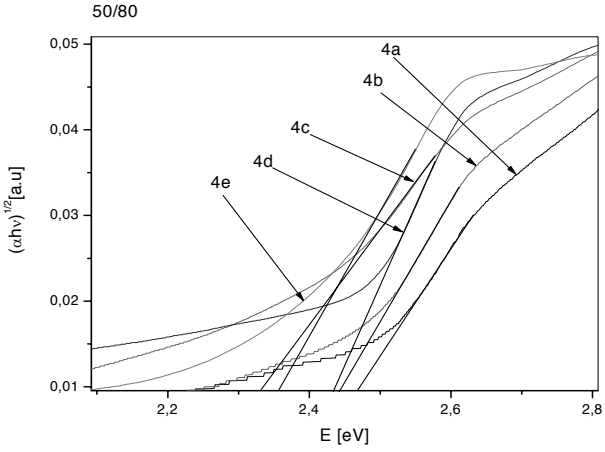

Fig. 15. Energy gaps E_g of PPI thin films

The values of energy gaps Eg of all PPI thin films were deduced with linear approximation (Fig. 15), known as Tauc relation [10]:

$$(\alpha \cdot E)^{1/2} = C(E - Eg) \quad (4)$$

where α is absorption coefficient and Eg is absorption gap. Values of conescutive Eg are shown in Table 4.

Table 3.
Values of RMS coefficients, growth rates V, and films thickness l

		a (I=0.05 Tr*l/s)			b (I=0.15 Tr*l/s)			c (I=0.4 Tr*l/s)			d (I=1 Tr*l/s)			e (I=3 Tr*l/s)		
No.	T_1/T_2	l	RMS	V	l	RMS	V	l	RMS	V	l	RMS	V	l	RMS	V
		[nm]	[nm]	[A/s]	[nm]	[nm]	[A/s]	[nm]	[nm]	[A/s]	[nm]	[nm]	[A/s]	[nm]	[nm]	[A/s]
1	50/50	29	3.74	2.38	136	3.24	11.13	221	4.69	18.41	393	4.91	32.67	496	4.42	39.17
2	50/60	183	2.06	19.49	274	7.65	29.58	517	6.4	55.21	660	3.69	71.02	720	6.64	77.58
3	50/70	131	3.65	15.99	206	5.92	25.33	517	25.93	63.19	781	25.93	95.36	892	4.64	109.69
4	50/80	260	4.83	25.69	338	7.65	32.35	615	4.29	60	1040	3.94	100.83	1696	18.82	164.23

Table 4.
Locations of individual absorption bands maxima and Eg values

	a)	b)	c)	d)	e)
	Eg	Eg	Eg	Eg	Eg
1	2.6	2.38	2.38	2.29	2.29
2	2.39	2.38	2.29	2.26	2.25
3	2.48	2.46	2.32	2.40	2.40
4	2.47	2.44	2.24	2.33	2.35

One can see, that values of energy gap are in range 2.24 – 2.48 eV.It easy seen, that there is generally tendency energy gap E_g decreasing with increment of growth rate V.

5. Conclusions

The polyazomethine thin films were prepared under different technological conditions of LCVD process. While preparing PPI thin films such parameters as gas stream intensity, I, and monomer's temperature difference, ΔT were changed. The UV – Vis optical absorption spectra and AFM microscope topographic images were presented. The LCVD parameters influence rate of thin film's growth V. It is easy seen, that rate V depend on gas stream intensity I and ΔT. The impact of this parameter is visible in optical spectra of thin PPI films prepared with the highest V.

The shift of bands gravity center with increase of I is connected with formation of longer conjugated fragments in polymer chains and their aggregation. The ordering of polymer structure and flattening of polymer chains are connected with stronger interactions between neighbour chains. The Wannier – Mott exciton is seen as sharp peak at 2.62 eV overlapping the lowest energy absorption band. This Wannier- Mott exciton is attributed to electrostatic connection between delocalised holes and delocalised electrons. The presence of Wannier exciton is connected with formation of more ordered areas in polymer and aggagation of polymer chains is possible.

Growth rate of thin films V influences morphology of polymer surface. Scattered big grains and holes are seen in surface of PPI thin films deposited with higher growth rate V.

The average diameter of grains is 0.18 μm, and average diameter of single big grains is 0.72 μm. Average depth of holes is 15 – 40 nm.

Active layer should be possible plain, devoid of holes and big grains in surface. These defects of layer morphology could be contribution of short circuit in optoelectronic structure (e.g. OLED) [16-19].

Acknowledgements

This paper has been done within the frame of the Project of Polish Ministry of Science and Education No N N507 4131 33.

References

[1] A. Kubono, N. Okui, Polymer thin films prepared by vapour deposition, Progress Polymer Science 19 (1994) 389-438.
[2] J. Mc Elvain, S. Tatsuura, F. Wudl, A.J. Heeger, Linear and nonlinear optical spectra of polyazomethines fabricated by chemical vapour deposition, Synthetic Metals 95 (1998) 101-105.
[3] W.R. Salaneck, R.H. Friend, J.L. Bredas, Electronic structure of conjugated polymers: consequences of electron-lattice coupling, Physics Reports 319 (1999) 231-251.
[4] M.S. Weaver, D.D.C. Bradley, Organic elektroluminescence devices fabricated with chemical vapour deposited polyazomethine films, Synthetic Metals 61-66 (1996) 83.
[5] L.A. Dobrzański, Engineering materials and materials design. Fundamentals of materials science and physical metallurgy, WNT, Warsaw-Gliwice, 2006 (in Polish).
[6] L.A. Dobrzański, D. Pakuła, Comparison of the structure and properties of the PVD and CVD coatings deposited on nitride tool ceramics, Proceedings of the 13th Scientific International Conference „Achievements in Mechanical and Materials Engineering" AMME'2005, Gliwice–Wisła, 2005 (CD-ROM).
[7] W. Kwaśny, D. Pakuła, M. Woźniak , L.A. Dobrzański, Fractal and multifractal characteristics of CVD coatings onto the nitride tool ceramics, Journal of Achievements in Materials and Manufacturing Engineering 20 (2007) 371-374.
[8] K.G. Basava Kumar, P.G. Mukunda, M. Chakraborty, Influence of melt treatments and polished CVD diamond-coated insert on cutting force and surface integrity in turning of Al-12Si and Al-12Si-3Cu cast alloys, International Journal of Manufacturing Research 2 (2007) 117-137.
[9] A. Jarząbek, J. Weszka, M. Domański, J. Cisowski, Optical properties of amorphous polyazomethine thin films, Journal of Non-Crystalline Solids 352 (2006) 1660-1662.
[10] B. Jarząbek, J. Weszka, M. Domański, J. Jurusik, J. Cisowski, Optical studies of aromatic polyazomethine thin films, Journal of Non-Crystalline Solids 354 (2008) 856-862.
[11] B.Hajduk, J.Weszka, B.Jarząbek, J.Jurusik, M.Domański, Physical properties of polyazomethine thin films doped with iodine, Jounal of Achievements in Materials and Manufacturing Engineering 24/1 (2007) 67-70.
[12] J. Jaglarz, J. Cisowski, H. Czternastek, W. Odsterczył, J. Jurusik, M. Domański, Diffuse scatering in polyazomethine thin films, Polymers 54/1 (2009) 15-18.
[13] F. Rohlfing, D.D.C. Bradley, Non linear Starc effect in polyazomethine and poly (p-phenylene-vinylene): The interconnections of chemical and electronic structure, Chemical Physics 227 (1998) 133-151.
[14] Y. Shimoi, S. Abe, Theory on electroabsorption in poly(p-phenylene vinylene), Synthetic Metals 91 (1997) 363-365.
[15] A. Borgesi, G. Tallarida, G. Amore, F. Cazzaniga, F. Queirolo, M. Alessandri, A. Sassela, Influence of roughness and grain dimension on the optical functions of polycrystalline silicon films, Thin Solid Films 313-314 (1998) 243-247.
[16] B. Walker, A. Kambili, S.J. Martin, Electrical transport modelling in organic electroluminescent devices, Journal of Physics: Condensed Matter 14 (2002) 9825-9876.
[17] W.R. Salaneck, R.H. Friend, J.L. Bredas, Electronic structure of conjugated polymers: Consequences of electron – lattice coupling, Physics Reports 319 (1999) 231-251.
[18] A. Schouwink, A.H. Schafer, C. Seidel, H. Fuchs, The influence of molecular aggregation on the device properties of organic light emitting diodes, Thin Solid Films 372 (2000) 163-168.
[19] D.D.C. Bradley, M. Grell, A. Grice, A.R. Tajbakhsh, D.F. O'Brien, A. Bleyer, Polymer light emission: control of properties through chemical structure and morphology, Optical Materials 9 (1998) 1-11.